Hand

Saira Haque

Introduction

Significant variations in the sizes of the bones in the hand, and relative portions of the ossified bone, occur in children of different ages. Motion artefact and suboptimal positioning can occur due to difficulty in keeping the hand still, particularly following significant injury. Failure to straighten the digits prevents clear definition of the joint spaces. Parents or caregivers may hold the child's hand flat and help placing items adjacent to the child's hand to obtain optimal imaging.

Skeletal Development of the Hand

- Skeletal maturity occurs in a specific pattern over a predictable timeline which is determined by [1]:
  (a) Development of ossification centres.
  (b) Level of calcium accumulation.
  (c) Bone structure and dimension.

S. Haque (✉)
King's College Hospital NHS Foundation Trust, London, UK
e-mail: saira.haque@nhs.net

P. Simoni, M. P. Aparisi Gómez (eds.), *Essential Measurements in Pediatric Musculoskeletal Imaging*,
https://doi.org/10.1007/978-3-031-17735-4_7

- Rate, duration and amount of growth and maturation vary widely.
- Females, at any age, have advanced bone age compared to males and this is more marked following pubertal onset.
- Epiphyseal region closes approximately 2 years earlier in girls.
- Skeletal maturation lasts longer in males [2].

Carpal Bone Ossification

- Carpal bones are not ossified at birth (Fig. 1).

FIGURE 1 Hand radiograph in a 1-month-old neonate demonstrates lack of ossification of the carpal bones

Table 1 Lists the mean age of ossification centre appearance in this order: capitate (1), hamate (2), triquetrum (3), lunate (4), trapezium (5), trapezoid (6), scaphoid (7) and pisiform (8)

Carpal bone	
Capitate	1–3 months
Hamate	2–4 months
Triquetrum	2–3 years
Lunate	2–4 years
Trapezium	4–6 years
Trapezoid	4–6 years
Scaphoid	4–6 years
Pisiform	8–12 years

- Significant variation in carpal development due to varying order of appearance, bone fusion or partitioning and development of accessory elements from cartilage [3].
- Approximately one ossification centre appears per year, up to the age of 7 years, except for the pisiform, which as a sesamoid appears during adolescence (Table 1).

Determination of Skeletal Maturity

- The hand and wrist have bones that develop over a clearly defined timeframe and can be easily assessed on a single posterior-anterior radiograph.
- These are key predictors which can aid the determination of skeletal maturity dependent on age [3]:
  1. Infancy (carpal bones and radial epiphyses).
  2. Toddler (number of epiphyses visible in long bones of the hand—Fig. 2).
  3. Prepuberty (ossification centres for phalangeal epiphyses are as wide as metaphyses and increase in thickness—Fig. 3).
  4. Early and mid-puberty (size of phalangeal epiphyses and epiphyses begin to overlap the metaphyses—Fig. 4).

Figure 2 Hand radiograph in a 3-year-old male demonstrates ossification of the capitate and hamate

5. Late puberty (fusion of epiphyses to metaphyses in the long bones of the hand in this order: distal phalanges [first], metacarpals [second], proximal phalanges [third] and finally fusion of middle phalanges).
6. Post-puberty (extent of epiphyseal fusion of radius and ulna).

FIGURE 3 Hand radiograph in a 5-year-old male demonstrates ossification centres for phalangeal epiphyses are becoming as wide as the metaphyses

Figure 4 Normal radiograph in a 13-year-old female showing that the phalangeal epiphyses begin to overlap the metaphyses

- Most common technique used to determine the level of bone maturation of the nondominant hand (in years) is Greulich and Pyle (G&P).
- Chronological age (in years) is determined from the child's birth date.
- Observers are more likely to interpret the radiograph as normal when chronologic age is known than when it is not.
- Ultrasound can be used to assess endochondral ossification and is of particular use to assess growth by assessment of distal radial and ulna epiphysis, using gender- and ethnicity-based algorithms [4].
- Magnetic resonance (MR) imaging is useful in growth assessment as it allows accurate assessment of the tubular and carpal bones.
- Epiphyseal cartilage, morphological appearance and size of the epiphyses, physeal structure/closure (bone bridges), zone of provisional calcification and progression of ossification are well assessed using MR imaging [5].

Carpal Angle

- Defined as the angle between:
  (a) Line from proximal surface of the scaphoid and lunate.
  (b) Line through the proximal triquetrum and lunate.

Normal value = 130°.

Increased (>139°): trisomy 21 and Pfeiffer syndrome.

Decreased (<118°): Hurler's syndrome, Morquio syndrome and Madelung deformity (Fig. 5).

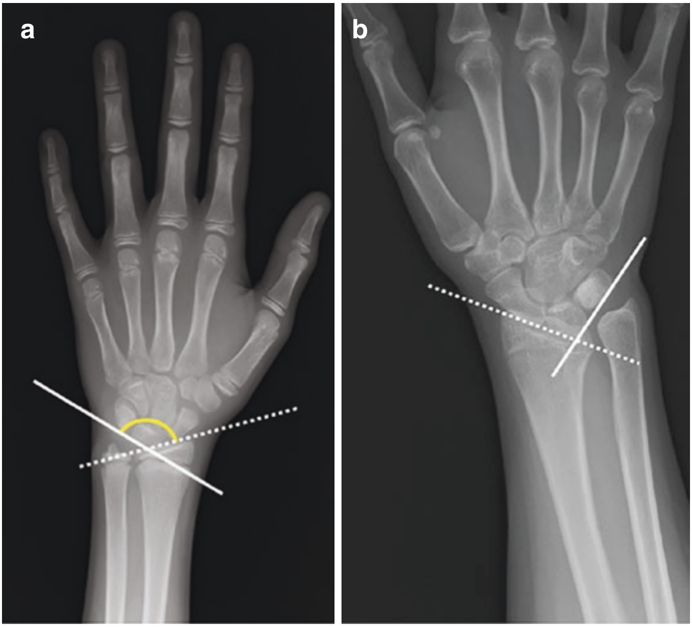

FIGURE 5 (**a**) Normal carpal angle, measured between the line from the proximal surface of the scaphoid and lunate (white dotted line) to the line through the proximal triquetrum and lunate (white bold line). (**b**) Reduced carpal angle in a case of Madelung deformity

Carpal Height

- Defined by the distance between the midpoint of the distal radial epiphysis ossification center and the proximal end of the third metacarpal [6].
- Useful in assessing congenital malformations, particularly when the carpus is not fully ossified.
- Carpal height increases as the child gets older.

- Carpal height ratio in children is similar to that seen in adults [7].
- The normal range of the carpal height ratio (calculated by dividing the carpal height by the length of the third metacarpal) is between 0.51 and 0.57 [8].
- Shortening of the carpus: multiple epiphyseal dysplasia, otopalatodigital syndromes, Turner syndrome, arthrogryposis and juvenile idiopathic arthritis (Figs. 6 and 7).

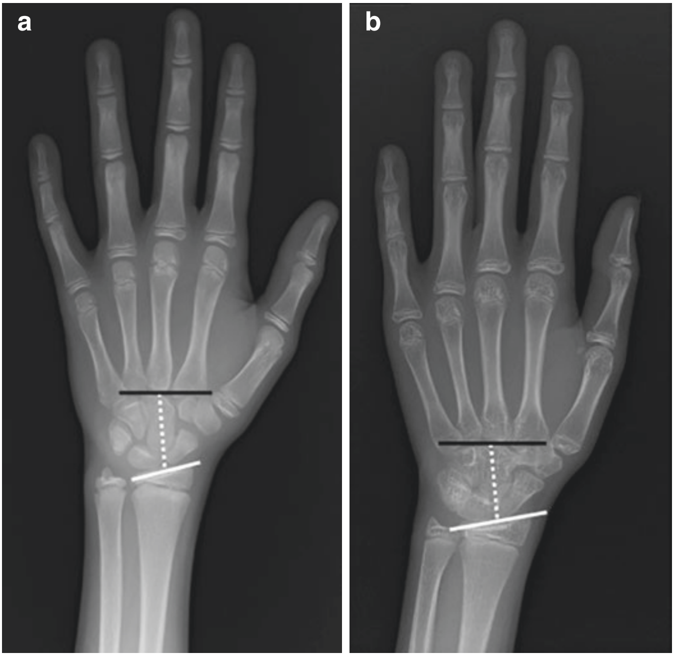

FIGURE 6 (**a**) The carpal height (white dotted line) is the distance between the midpoint of the distal radial epiphyseal ossification center (white line) and proximal end of the third metacarpal (black line). This is reduced due to carpal crowding in a 13-year-old (**b**)

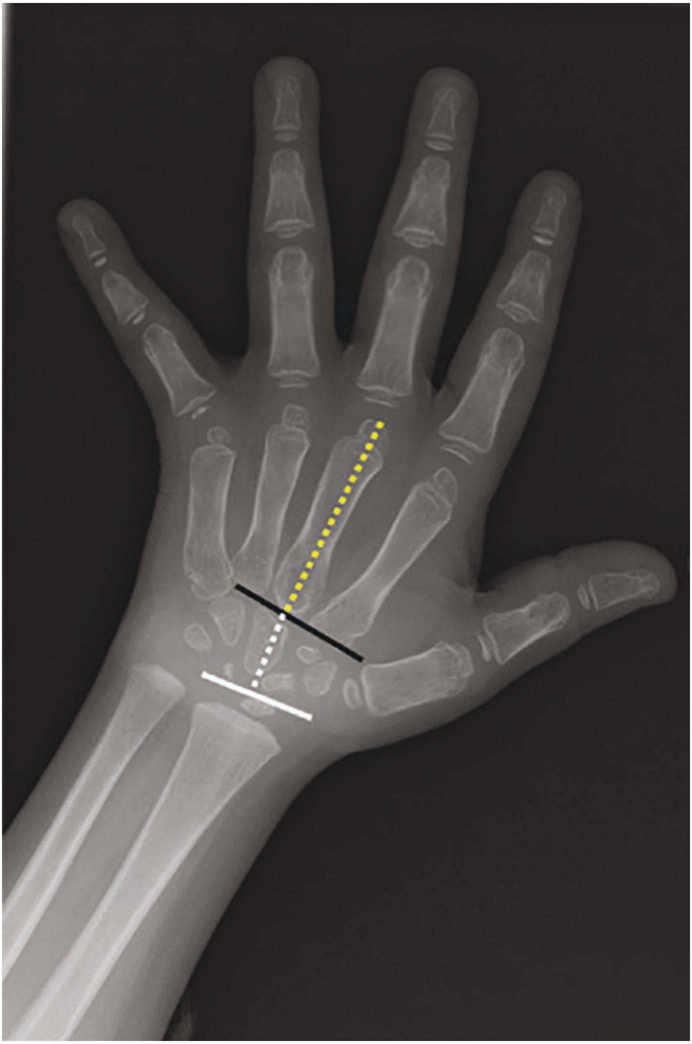

Figure 7 7-year-old with spondyloepiphyseal dysplasia. Reduction in carpal height due to hypoplasia of the carpal bones; the carpal height ratio has been calculated by dividing the carpal height (white dotted line) by the length of the third metacarpal (yellow dotted line). The midpoint of the distal radial epiphyseal ossification center is indicated by the white line and the proximal end of the third metacarpal depicted by the black line

Scapholunate Distance

- Scapholunate distance of less than or equal to 2 mm is used to assess for soft tissue injuries in adults [9].
- In younger children, this distance is normally wider due to the larger chondral component of the scaphoid and lunate, and this decreases with age [10].
- Boys have a longer distance than girls due to earlier skeletal maturity and develop adult values from 12 years of age (Figs. 8 and 9).
- Mean Scapholunate Distance According to Age [11]
  6 Years: 7–9 mm
  7 Years: 6–8 mm
  8 Years: 5.5–7.5 mm
  9 Years: 5–6.5 mm
  10 Years: 4.5–6 mm
  11 Years: 4–5 mm
  12 Years: 3.5–4.5 mm

FIGURE 8 12-year-old male with a scaphoid waist fracture and widening of the scapholunate distance (dotted yellow line) secondary to a scapholunate ligamentous injury

FIGURE 9 Coronal CT image of a 15-year-old male with significant widening of the scapholunate distance (dotted yellow line) measuring 10 mm; incidental note of lunotriquetral coalition

Carpal Instability

- Scapholunate and capitolunate angles can be used on lateral radiographs or sagittal imaging to assess carpal instability.
- This is possible when the carpal bones are ossified appropriately, for example, when the proximal and distal poles of the scaphoid are discernible [12].
- Capitolunate angle: angle between the long axis of the capitate and the mid-axis of the lunate.
- Mean capitolunate angle is 11° (SD ± 7°).

- This angle is increased in dorsal intercalated segment instability and volar intercalated segment instability; the scapholunate angle is used to differentiate between these two entities.
- Scapholunate angle: angle between line drawn through the axis of the scaphoid and lunate.
- Mean scapholunate angle is 47° (SD ± 8), and if this angle is >80°and the lunate is extended, features are suggestive of dorsal intercalated segmental instability.

Metacarpal Index

- This is a measure of the slenderness of the metacarpals.
- Metacarpal index increases from lower values in early childhood to adult range by 10 to 11 years in normal children [13].
- Ratio of mean length to mean width of second to fifth metacarpals, measured at their midpoints.
- A second method involves dividing the sum of the lengths by the sum of the widths of the metacarpals.
- Normal metacarpal index <7–9 (Fig. 10) but in arachnodactyly it is >8.5 (metacarpals are longer and thinner than normal).
- Arachnodactyly is associated with Marfan syndrome, osteogenesis imperfecta, dystrophia myotonica, homocystinuria and Ehlers-Danlos syndrome [14].
- It is important to note that the metacarpal index is a poor discriminator of patients with tall stature or clinical signs of arachnodactyly; these patients should still be examined for additional signs of Marfan syndrome or other inherited disorders of connective tissue.

FIGURE 10 Metacarpal index in a 13-year-old girl, within the normal range (value was 7). The metacarpal index is determined by dividing the length of each of the last four metacarpals (white lines) by the width of the midpoint (black lines) and averaging the values

Metacarpal Sign

- Assesses the lateral three metacarpals by drawing a tangential line along the distal fifth and fourth metacarpals.
- Normally, this passes distal to the head of the third metacarpal, but if this intersects the third metacarpal, the fourth metacarpal is considered short.
- Can be seen as normal variant, Turner syndrome, pseudohyperparathyroidism, acrodysostosis and occasionally homocystinuria (Fig. 11).
- This sign is negative if all metacarpals are short or if there is greater shortening of the third metacarpal than the fourth metacarpal [15].

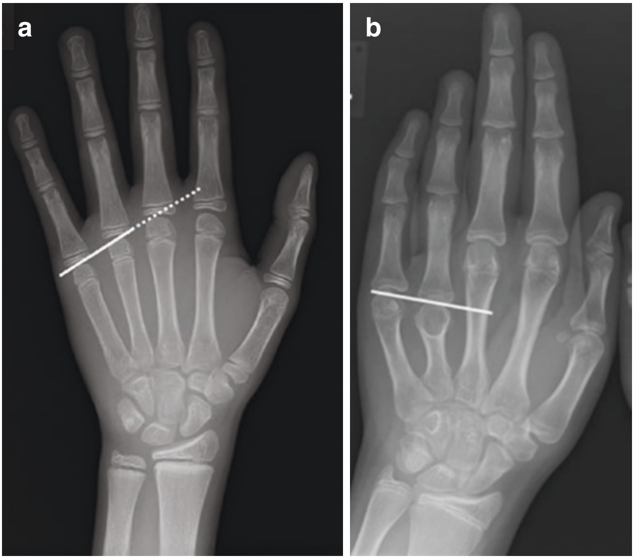

FIGURE 11 In image (**a**), a tangential line drawn along distal fifth and fourth metacarpals (white line) passes distal to head of the third metacarpal (dotted line). In image (**b**), the tangential line (white line) drawn along distal fifth and fourth metacarpals extends to the mid-shaft of the third metacarpal in a patient with Turner syndrome

Brachydactyly

- Congenital: shortened hands due to absence or rudimentary development of metacarpals and/phalanges; inherited (usually dominant trait) but can be part of a syndrome (Fig. 12).
- PA view of the hands is the first-line investigation.
- Brachyphalangy (abnormal short phalanges), brachybasophalangia (proximal), brachymesophalangia (middle) and brachytelephalangia (distal).

FIGURE 12 This image of a 5-year-old patient with mucopolysaccharidosis (MPS) type IV demonstrates brachydactyly with widened and shortened tubular bones, shortening of the metacarpals, pointing of the second through fifth metacarpals and irregular carpal bones

- Most used index of digit length: ratio of middle finger (cm) to hand length (cm)—measured with hand open from fingerprint to the principal crease where finger joins the palm and the palm joins the wrist; middle finger length (50th centile): 5 cm (4 years), 6 cm (8 years), 7 cm (12 years) and 8 cm (16 years) [16].

Joint Fluid

- Even small effusions (1 mm) can be detected in the hand joints with an interobserver agreement of 79% using ultrasound [17].
- Dorsal recesses are measured using ultrasound in a mid-sagittal view.
- The hand is kept in a neutral position as flexion leads to reduction or disappearance of the fluid (Fig. 13).
- Mean depth of radiocarpal recess = 0.4 mm (SD 0.5, range 0–2.9) [18].
- Mean depth of midcarpal recess = 0.5 mm (SD 0.6, range 0–2.4).

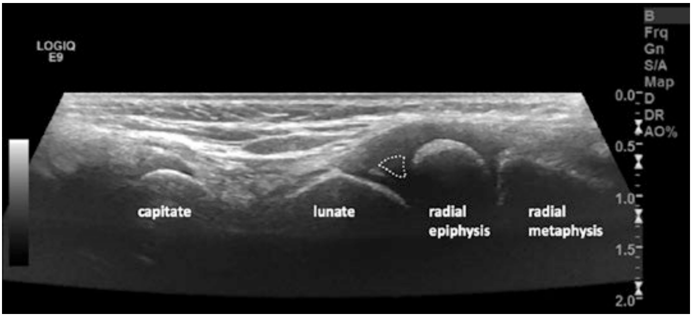

Figure 13 Dorsal recess (outlined in dotted line) of the radiocarpal joint has been measured using ultrasound in the mid-sagittal view

- No differences according to sex, but increasing depth of the recesses by age.
- One or more vessels are seen in 8% of the radiocarpal and 4% of the midcarpal recesses (Fig. 14).
- There is a considerable variation in normal synovial thickness, up to 5 mm [19] (Fig. 15).

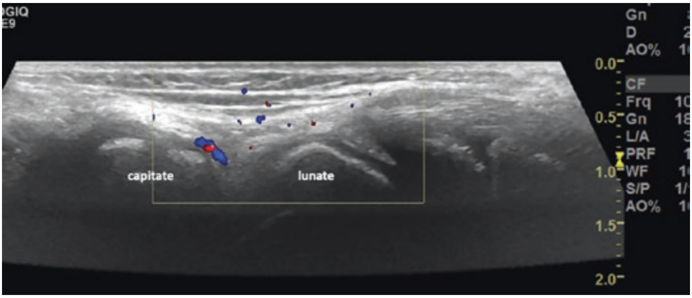

FIGURE 14 Mid-sagittal view of the midcarpal joint using ultrasound demonstrates a normal vessel

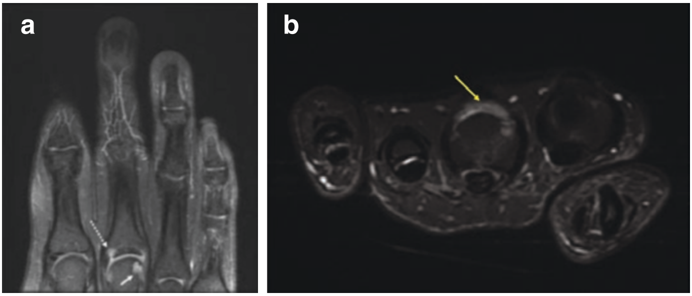

FIGURE 15 This coronal (**a**) and axial (**b**) STIR MR images in an 11-year-old girl demonstrate joint fluid in the middle finger metacarpal joint, synovial proliferation (yellow arrow in the axial view), and erosions at the metacarpal head (white arrow in the coronal view) and proximal phalanx of the middle finger (dotted arrow in the coronal view)

Tendon Pathology

- There is a strong linear relationship between tendon thickness and age, with the tendon thickness increasing with age.
- Minimal fluid (0.3 mm) can be seen in the tendon sheaths of children; a hypoechoic rim can be detected around the finger tendon sheath particularly on the palmar aspect of the metacarpal [20].
- Ultrasound is superior to MRI in depicting dynamic pathology and allowing comparison with the opposite side (Fig. 16).

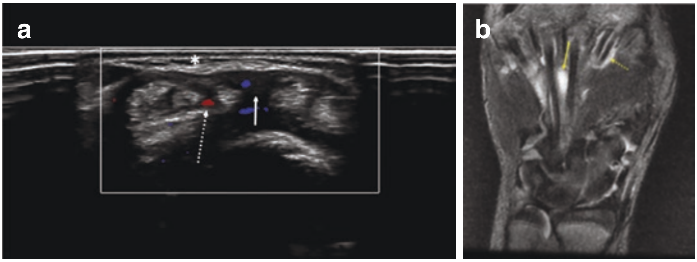

FIGURE 16 4-year-old who presented with hand swelling. Transverse ultrasound image (**a**), with colour Doppler flow, demonstrates thickening of the synovial sheath (8 mm thickness) of the extensor digitorum tendons (white arrow), increased vascularity (dotted arrow) and peritendinous subcutaneous oedema (asterisk). Coronal STIR image on MR (**b**) performed subsequently also demonstrates fluid (yellow arrow) and synovial thickening (dotted yellow arrow) surrounding the extensor digitorum tendons

Paediatric Trigger Thumb

- Results in abnormal flexion at the interphalangeal joint due to thickening of the flexor pollicis longus tendon (secondary to abnormal synovial proliferation, collagen degeneration).
- Triggering occurs when the cross-sectional area of the flexor pollicis longus exceeds the cross-sectional area demarcated by the A1 pulley (Fig. 17); unilateral triggering and a trigger ratio (maximal cross-sectional area of involved FPL to uninvolved FPL) <1.5 are at risk for developing triggering bilaterally [21, 22].

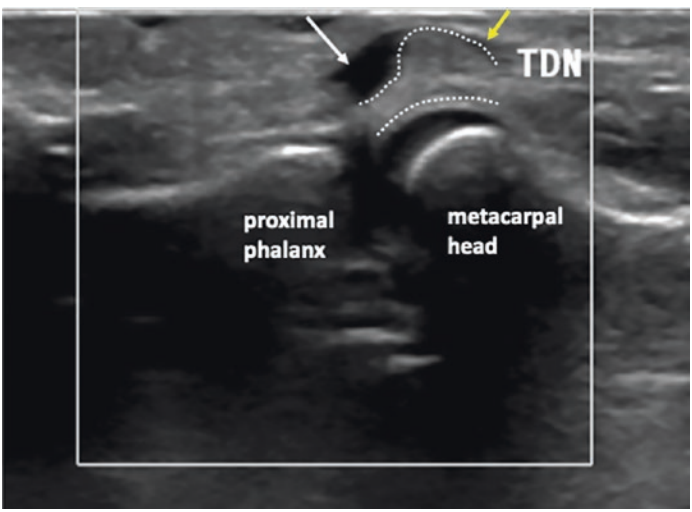

FIGURE 17 Longitudinal ultrasound image in an 11-month-old demonstrates the metacarpal joint of the thumb with developmental mismatch between the thickened FPL tendon (yellow arrow) and the area under the A1 pulley (white arrow)

Carpal Tunnel

- Carpal tunnel syndrome is best assessed by looking at the median nerve echogenicity, proximal to the retinaculum flexorum, and by identifying the site of greatest nerve enlargement.
- Wrist-to-forearm ratio of proximal and distal cross-sectional area measurement of the median nerve is also helpful for assessment [23] (Fig. 18). Wrist-to-forearm ratio in normal circumstances approaches 1. In carpal tunnel syndrome, there is thickening of the nerve at the wrist.
- Prominent signs of carpal tunnel syndrome include hypoechogenicity or a wrist-to-forearm ratio >1.5.
- Moderate signs of carpal tunnel syndrome include hypoechogenicity and a wrist-to-forearm ratio >2.

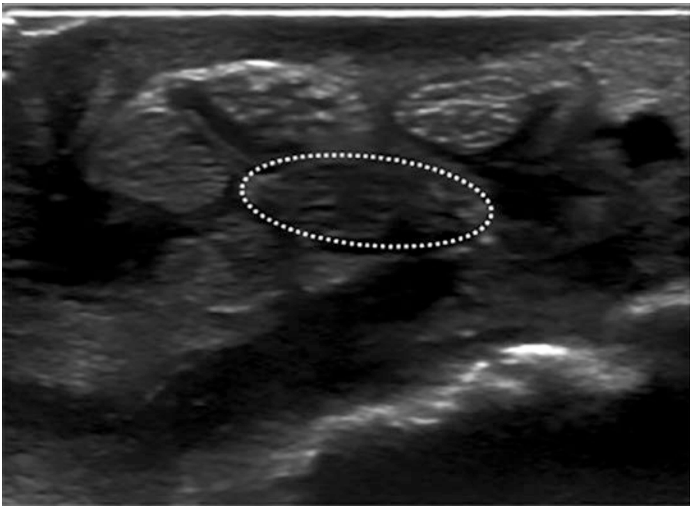

Figure 18 Transverse ultrasound image of the right median nerve (outlined) at the level of the carpal tunnel, proximal to the retinaculum flexorum, in a 9-year-old female, demonstrates enlargement and reduced echogenicity consistent with carpal tunnel syndrome

References

1. Tanner JM, Whitehouse RH. Growth at adolescence. 2nd ed. Springfield, IL: Blackwell Scientific; 1962.
2. Mora S, Boechat MI, Pietka E, Huang HK, Gilsanz V. Skeletal age determinations in children of European and African descent: applicability of the Greulich and Pyle standards. Pediatr Res. 2001;50:624–8. https://doi.org/10.1203/00006450-200111000-00015.
3. Cavallo F, Mohn A, Chiarelli F, Giannini C. Evaluation of bone age in children: a mini-review. Front Pediatr. 2021;9:580314. https://doi.org/10.3389/fped.2021.580314.
4. Mentzel HJ, Vilser C, Eulenstein M, et al. Assessment of skeletal age at the wrist in children with a new ultrasound device. Pediatr Radiol. 2005;35:429–33. https://doi.org/10.1007/s00247-004-1385-3.
5. Tomei E, Sartori A, Nissman D, Al Ansari N, Battisti S, Rubini A, Stagnitti A, Martino M, Marini M, Barbato E, Semelka RC. Value of MRI of the hand and the wrist in evaluation of bone age: preliminary results. J Magn Reson Imaging. 2014;39(5):1198–205. https://doi.org/10.1002/jmri.24286. PMID: 25006631
6. Poznanski AK, Hernandez RJ, Guire KE, Bereza UL, Garn SM. Carpal length in children—a useful measurement in the diagnosis of rheumatoid arthritis and some concenital malformation syndromes. Radiology. 1978;129(3):661–8. PMID: 725041. https://doi.org/10.1148/129.3.661.
7. Sallam AA, Briffa N, Mahmoud SS, Imam MA. Normal wrist development in children and adolescents: a geometrical observational analysis based on plain radiographs. J Pediatr Orthop. 2020;40(9):e860–72. PMID: 32404657. https://doi.org/10.1097/BPO.0000000000001584.
8. Youm Y, McMurthy RY, Flatt AE, Gillespie TE. Kinematics of the wrist. I. an experimental study of radial-ulnar deviation and flexion-extension. J Bone Joint Surg Am. 1978;60(4):423–31. PMID: 670263.
9. Okan N, Caboğlu F, Mertoğlu T, Durakbaşa O, Görgeç M. Cocuklarda the measurement of wrist kinematics in children 4 to 16 years old and the comparison of the scapholunate distance with adult values. Acta Orthop Traumatol Turc. 2004;38(1):30–3. PMID: 15054295.

10. Kaawach W, Ecklund K, Di Canzio J, Zurakowski D, Waters PM. Normal ranges of scapholunate distance in children 6 to 14 years old. J Pediatr Orthop. 2001;21(4):464–7.
11. Leicht P, Mikkelsen B, Larsen CF. Scapholunate distance in children. Acta Radiol. 1996;37(5):625–6.
12. Joyce EA, Farrell T, McMorrow J, et al. Are adult carpal angle measurements applicable to the pediatric population in the trauma setting? Skeletal Radiol. 2018;47:1151–6.
13. Rand TC, Edwards DK, Bay CA, et al. The metacarpal index in normal children. Pediatr Radiol. 1980;9:31–2. https://doi.org/10.1007/BF00973966.
14. Nelle M, Tröger J, Rupprath G, Bettendorf M. Metacarpal index in Marfan's syndrome and in constitutional tall stature. Arch Dis Child. 1994;70(2):149–50. https://doi.org/10.1136/adc.70.2.149.
15. Poznanski AK. Useful measurements in the evaluation of hand radiographs. Hand Clin. 1991;7(1):21–36. PMID: 2037636.
16. Normogram can be found in the Appendix of Jones, ed. Smith's recognizable patterns of human malformation, 5th ed. Philadelphia: Saunders; 1997. [Sivan Y, Merlob P, Reisner SH. Upper Limb Standards in Newborns. Am J Dis Child. 1983;137(9):829–32]. https://doi.org/10.1001/archpedi.1983.02140350007003.
17. Szkudlarek M, Court-Payen M, Jacobsen S, Klarlund M, Thomsen HS, Ostergaard M. Interobserver agreement in ultrasonography of the finger and toe joints in rheumatoid arthritis. Arthritis Rheum. 2003;48:955–62. https://doi.org/10.1002/art.10877.
18. Rosendahl K, Bruserud IS, Oehme N, et al. Normative ultrasound references for the paediatric wrist; dorsal soft tissues. RMD Open. 2018;4:e000642. https://doi.org/10.1136/rmdopen-2017-000642.
19. Smith MD. The normal synovium. Open Rheumatol. 2017;12:63.
20. Collado P, Naredo E, Calvo C, Crespo M. Assessment of the joint recesses and tendon sheaths in healthy children by high-resolution B-mode and power Doppler sonography. Clin Exp Rheumatol. 2007;25(6):915–21. PMID: 18173930.
21. Verma M, Craig CL, DiPietro MA, Crawford J, VanderHave KL, Farley FA, Caird MS. Serial ultrasound evaluation of pediatric trigger thumb. J Pediatr Orthop. 2013;33(3):309–13. PMID: 23482269. https://doi.org/10.1097/BPO.0b013e318287f728.

22. Kim J, Gong HS, Seok HS, Choi YH, Oh S, Baek GH. Quantitative measurements of the cross-sectional configuration of the flexor pollicis longus tendon using ultrasonography in patients with pediatric trigger thumb. J Hand Surg Am. 2018;43(3):284.e1–7. Epub 2017 Sep 19. https://doi.org/10.1016/j.jhsa.2017.08.011.
23. Descatha A, Huard L, Aubert F, Barbato B, Gorand O, Chastang JF. Meta-analysis on the performance of sonography for the diagnosis of carpal tunnel syndrome. Semin Arthritis Rheum. 2012;41(6):914–22.